There is much less reported data on relative success rates in different races for intracranial B mode imaging. Asian populations have a high frequency of poor temporal bone windows (TBWs) [8–10]; failure to detect the sphenoidal portion of the middle cerebral artery (M1) on TCCS could be secondary to M1 occlusion or to an inadequate TBW, or sometimes to poor technique or wrong gain settings. The hyperechoic lesser sphenoid wing and superior margin of the petrous pyramid were proposed to be indicators for the identification of the middle and posterior cerebral arteries [11]. This study aimed to clarify the relationship between visibilities of the contralateral temporal bone (CTB), midbrain (MB) and ipsilateral lesser sphenoid wing (LSW) on B mode images and the detectability of the ipsilateral M1 on color Doppler images by TCCS. We have attempted to develop a simple indicator to determine whether failure to detect flow in the M1 is secondary to local arterial disease or to an inadequate bone window.

Subjects and Methods

Consecutive patients with acute ischemic stroke admitted to our stroke center within 7 days after stroke onset between January 2009 and July 2009 were prospectively registered. They were evaluated by intracranial magnetic resonance imaging (MRI) for brain and intracranial magnetic resonance angiography (MRA) for intracranial arteries with a 1.5-tesla system (Magnetom Vision; Siemens, Germany), and carotid duplex ultrasonography for the common carotid artery and the extracranial internal carotid artery (ICA) using a Hitachi EUB-8500 ultrasound machine (Hitachi Medical Corp, Tokyo, Japan) with a 7.5-MHz linear probe on admission. Patients having an M1 or an ICA with luminal stenosis >50% or occlusion on baseline intracranial MRA or carotid ultrasonography, those having a pacemaker, or those who had an extracranial-intracranial arterial bypass were excluded from our study.

TCCS Examination

TCCS examination using a Hitachi EUB-8500 ultrasound machine with a 2- to 2.5-MHz sector probe was performed transtemporally in horizontal projection within 24 h after initial MRA and carotid US evaluations. Patients were lying in a supine, left lateral or right lateral decubitus position according to the side of the TBW examined and the patient's condition. With a scanning depth of 15.5 cm as a fixed depth, the CTB was visualized first for orientation, and the visibilities of the CTB, MB and LSW were assessed. On B mode images, the MB is hypoechoic and butterfly-shaped, and it is surrounded by hyperechoic subarachnoid cisterns, and the LSW has a hyperechoic outline of the bony structures at the skull base [11]. The B mode gain was initially set at 20 and adjusted to optimize structure delineation in the ultrasound image. Then color Doppler ultrasound was used to identify the intracranial arteries. The color gain was set at 38 as a default value and adjusted to obtain an optimum color display to the setting just below that in which background noise first becomes apparent. The velocity color scale was initially set at ±27.3 cm/s. To mitigate aliasing, color flow velocity settings were changed between ±2.3 and ±54.7 cm/s. The M1 at a depth of 4–6 cm was evaluated as a unidirectional flow toward the probe on color Doppler images. If color dots or discontinuous color were initially detected, whether the vessel was the M1 or not was judged based on the depth, the positional relationships with the probe and the intracranial structures, and the direction of blood flow, and further attempts to manipulate the probe superiorly and inferiorly to identify the remainder of the M1 were performed. If the MB and LSW could not be clearly identified, we carefully measured the intracranial head diameter by using the B mode and used the actual depth to guide the examination. Two experienced vascular neurologists who knew the information of the M1 on baseline MRA assessed the visibilities of the MB, LSW and CTB on B mode images and assigned patients into 4 categories as follows: 'invisible' if the hyperechoic CTB within the echo window, the peduncle of the MB or the hyperechoic LSW within the echo window was not visible at all; 'poor' if it was visible less than 50%; 'fair' if it was visible more than 50%, and 'good' if it was almost totally visible (fig. 1, 2). The detectability of the M1 was assessed on color Doppler images and assigned into similar categories as follows: 'INVISIBLE' if the M1 was undetected, 'POOR' if detected as color dots, 'FAIR' if linearly but discontinuously detectable and 'GOOD' for being linearly and continuously detectable (fig. 2, 3). When the M1 was assigned into the category 'INVISIBLE', the detectabilities of the anterior and posterior cerebral arteries from the same TBW were also evaluated to ascertain the absence of a proper TBW according to the recent consensus recommendations [4]. The posterior cerebral artery was detectable if the precommunicating segment, proximal or distal postcommunicating segment was detected. The interrater and intrarater agreements for each of the categories (invisible, poor, fair and good), by kappa statistic, were 0.45 and 0.64 for the MB, 0.62 and 0.85 for the LSW, 0.61 and 0.71 for the CTB, and 0.89 and 0.96 for the M1, respectively, according to the offline video monitoring evaluations of 20 randomly selected patients by the above-mentioned two experienced vascular neurologists.

Contrast-Enhanced TCCS Examination

Contrast-enhanced TCCS examination was performed in the initial 10 patients who had 'INVISIBLE', 'POOR' or 'FAIR' detection of the M1 on color Doppler images after they had given their informed consent. Levovist (Bayer Health Care, Leverkusen, Germany), an ultrasound contrast agent consisting of granules composed of 99.9% galactose and 0.1% palmitic acid, was used. Levovist was injected at a dose of 2.5 g diluted in 7 ml of 0.9% saline resulting in a concentration of 300 mg/ml (total volume, 8.5 ml). A 4.25-ml bolus of Levovist was injected into an antecubital vein within 10 s, followed by a 10-ml saline chaser bolus for the one side. A second injection for the other side was administered after the first contrast effect had faded out. Detectability improvement on contrast-enhanced TCCS examination was defined as improvement of M1 detectability on contrast-enhanced TCCS by one or more categories compared with that on non-contrast-enhanced examination.

Data Analysis

The percentages of each finding were calculated for all patients, by sex and by age (<70 years old or ≥70 years old). The percent-

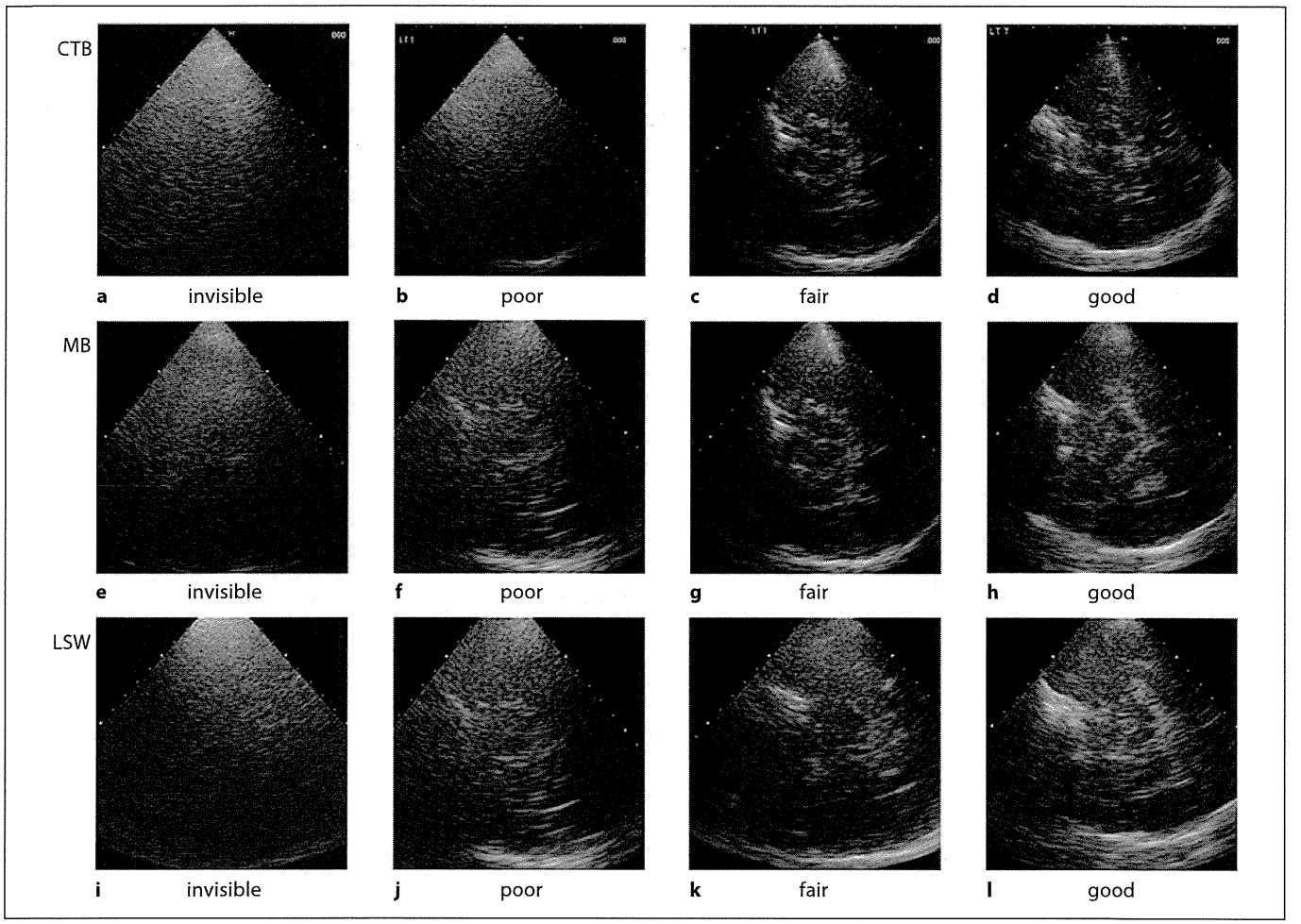

Fig. 1. Visibilities of CTB (**a–d**), MB (**e–h**) and LSW (**i–l**) on B mode images. invisible = The contour is not visible; poor = the contour is less than 50% visible; fair = the contour is more than 50% visible; good = the contour is almost totally visible.

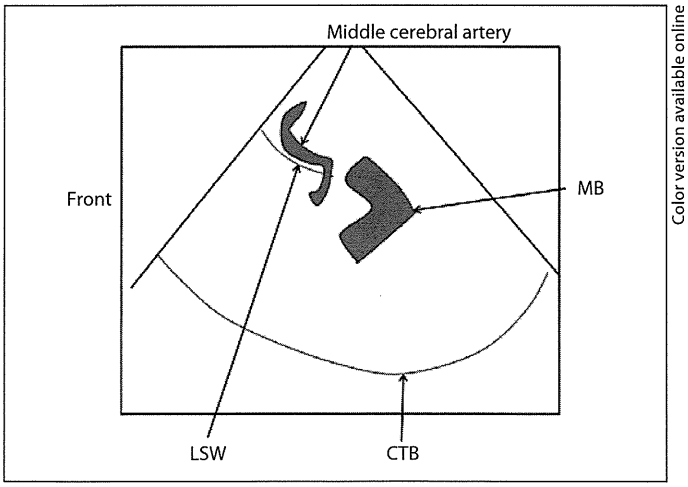

Fig. 2. A schema of CTB, MB, LSW and middle cerebral artery.

Color version available online

ages of each category were compared by sex and by age using the χ^2 test. The relationship between each structure's visibility and M1 detectability was analyzed using Spearman's rank correlation. The percentages of M1 detection improvement by categorical visibility of each structure on B mode images were calculated.

Results

One hundred and twenty-four acute ischemic stroke patients admitted to our stroke center during the study period were investigated. Forty-six patients who had vascular abnormality on MRA (13 ICA occlusion, 5 ICA stenosis ≥50%, 1 ICA pseudo-occlusion, 14 middle cerebral artery M1 occlusion, 13 middle cerebral artery M1 stenosis ≥50%), 1 patient having a pacemaker, and 1 patient

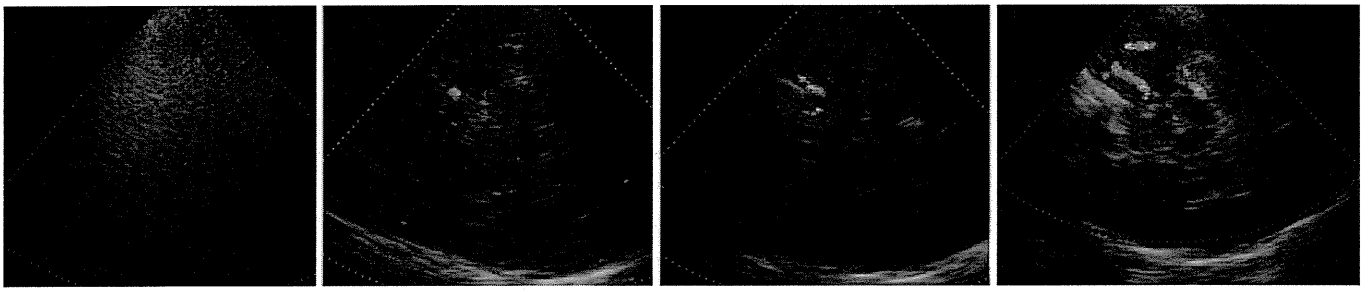

Fig. 3. M1 detectability on color Doppler images. **a** The M1 is undetectable (INVISIBLE). **b** The M1 is detected as color dots (POOR). **c** The M1 is linearly but discontinuously detectable (FAIR). **d** The M1 is linearly and continuously detectable (GOOD).

who had superficial temporal artery/middle cerebral artery anastomosis were excluded. Seventy-six patients (48 men, 71 ± 12 years old) with 152 TBWs were evaluated by TCCS. None of these had a large infarction which caused brain displacement on MRI. Table 1 summarizes the percentages of each structure's visibility on B mode images and M1 detectability on color Doppler images for all patients, by sex and by age. There were 38 TBWs of women aged ≥70 years, 42 TBWs of men aged ≥70 years, 18 TBWs of women aged <70 years and 54 TBWs of men <70 years. The CTB, MB and LSW were visible on B mode in 98, 64 and 84%, respectively; levels of visibility are shown in table 1. The M1 was detected in 49% on color Doppler images, and M1 detectability was 'POOR' in 7%, 'FAIR' in 7% and 'GOOD' in 35%. Structural visibilities on B mode and M1 detectability were better in men than in women and in younger adults (<70 years old) than in older adults (≥70 years old). Among 77 TBWs with an 'INVISIBLE' M1, the anterior cerebral artery was detectable only through 4 TBWs, and the PCA was detectable through 25 TBWs (table 2).

The correlation coefficient between each structure's visibility and M1 detectability was 0.68 for the CTB, 0.66 for the MB and 0.80 for the LSW ($p < 0.001$ for all; table 3). The M1 was detectable as 'GOOD' in 40 (82%) out of 49 TBWs with 'good' LSW visibility, although it was so in 43 (70%) out of 61 TBWs with 'good' CTB visibility and in 17 (77%) out of 22 TBWs with 'good' MB visibility. When the LSW was invisible, the M1 was not detected. When the LSW was less than 50% visible, the M1 was detected in 9%. When the LSW was more than 50% visible, the M1 was detected in 55%. When the LSW was almost totally visible, the M1 was detected in 98%. The correlation coefficients between each structure's visibility and M1 detectability in men were 0.62 for the CTB, 0.60 for the MB and 0.74 for the LSW ($p < 0.001$ for all); those in women were 0.58, 0.53 and 0.72, respectively ($p < 0.001$ for all). Those of younger adults were 0.61, 0.58 and 0.74, respectively ($p < 0.001$ for all); those of older adults were 0.71, 0.70 and 0.80, respectively ($p < 0.001$ for all).

Contrast-enhanced TCCS examination was performed in 20 TBWs of 10 patients (table 4). In 8 of 20 TBWs (40%), the M1 was identified with 1 or more category improvements compared with that on non-contrast-enhanced examination. The detection improvement of the M1 was ascertained for no TBWs with 'invisible' LSW, 50% with 'poor' LSW, 57% with 'fair' LSW and 50% with 'good' LSW.

Discussion

In this study, categorical visibilities of the CTB, MB and LSW on B mode images and categorical M1 detectability on color Doppler images by TCCS were determined in Japanese acute ischemic stroke patients without stenotic lesions of the M1 or ICA on baseline MRA or carotid ultrasonography. The major findings were as follows: first, the M1 was detectable by TCCS in 49% in this study of patients with a known patent M1. Second, visibilities of the CTB, MB and LSW on B mode images had positive correlations with M1 detectability on color Doppler images. Third, LSW visibility was a better indicator than CTB and MB visibilities for evaluation of the M1. Fourth, contrast-enhanced TCCS examination provided better M1 detection than nonenhanced examination in half of the TBWs through which each structure was vis-

Table 1. Structural visualization and M1 detectability by TCCS

Structural visualization on B mode image		invisible	visible			p
			poor	fair	good	
Structural visualization on B mode image						
CTB	Total (152 TBWs)	3 (2)	34 (22)	54 (36)	61 (40)	
	Women (56 TBWs)	3 (5)	25 (45)	16 (29)	12 (21)	<0.0001[a]
	Men (96 TBWs)	0	9 (9)	38 (40)	39 (51)	
	Aged ≥70 years (80 TBWs)	3 (4)	23 (29)	30 (38)	24 (30)	0.0163[b]
	Aged <70 years (72 TBWs)	0	11 (15)	24 (33)	37 (51)	
	Women aged ≥70 years (38 TBWs)	3 (8)	20 (53)	10 (26)	5 (13)	0.0689[c]
	Women aged <70 years (18 TBWs)	0	5 (28)	6 (33)	7 (39)	
	Men aged ≥70 years (42 TBWs)	0	3 (7)	20 (48)	19 (45)	0.3486[d]
	Men aged <70 years (54 TBWs)	0	6 (11)	18 (33)	30 (56)	
MB	Total (152 TBWs)	55 (36)	36 (24)	39 (26)	22 (14)	
	Women (56 TBWs)	37 (66)	10 (18)	7 (13)	2 (4)	<0.0001[a]
	Men (96 TBWs)	18 (19)	26 (27)	32 (33)	20 (21)	
	Aged ≥70 years (80 TBWs)	39 (49)	22 (28)	17 (21)	2 (3)	<0.0001[b]
	Aged <70 years (72 TBWs)	16 (22)	14 (19)	22 (31)	20 (28)	
	Women aged ≥70 years (38 TBWs)	30 (79)	6 (16)	2 (5)	0	0.0061[c]
	Women aged <70 years (18 TBWs)	7 (39)	4 (22)	5 (28)	2 (11)	
	Men aged ≥70 years (42 TBWs)	9 (21)	16 (38)	15 (36)	2 (5)	0.0046[d]
	Men aged <70 years (54 TBWs)	9 (17)	10 (19)	17 (31)	18 (33)	
LSW	Total (152 TBWs)	25 (16)	34 (22)	44 (29)	49 (32)	
	Women (56 TBWs)	15 (27)	23 (41)	10 (18)	8 (14)	<0.0001[a]
	Men (96 TBWs)	10 (10)	11 (11)	34 (35)	41 (43)	
	Aged ≥70 years (80 TBWs)	16 (20)	22 (28)	23 (29)	19 (24)	0.0700[b]
	Aged <70 years (72 TBWs)	9 (13)	12 (17)	21 (29)	30 (42)	
	Women aged ≥70 years (38 TBWs)	13 (34)	16 (42)	5 (13)	4 (11)	0.1649[c]
	Women aged <70 years (18 TBWs)	2 (11)	7 (39)	5 (28)	4 (22)	
	Men aged ≥70 years (42 TBWs)	3 (7)	6 (14)	18 (43)	15 (36)	0.3460[d]
	Men aged <70 years (54 TBWs)	7 (13)	5 (9)	16 (30)	26 (48)	
M1 detectability on color Doppler images		INVISIBLE	POOR	FAIR	GOOD	p
M1	Total (152 TBWs)	77 (51)	11 (7)	11 (7)	53 (35)	
	Women (56 TBWs)	42 (75)	3 (5)	2 (4)	9 (16)	<0.0001[a]
	Men (96 TBWs)	35 (36)	8 (8)	9 (9)	44 (46)	
	Aged ≥70 years (80 TBWs)	46 (58)	8 (10)	7 (9)	19 (24)	0.0198[b]
	Aged <70 years (72 TBWs)	31 (43)	3 (4)	4 (6)	34 (47)	
	Women aged ≥70 years (38 TBWs)	29 (76)	3 (8)	1 (3)	5 (13)	0.5002[c]
	Women aged <70 years (18 TBWs)	13 (72)	0	1 (6)	4 (22)	
	Men aged ≥70 years (42 TBWs)	17 (40)	5 (12)	6 (14)	14 (33)	0.1146[d]
	Men aged <70 years (54 TBWs)	18 (33)	3 (6)	3 (6)	30 (56)	

Values are represented by numbers of TBWs, with percentages in parentheses.
[a] Women versus men by χ^2 test. [b] Aged ≥70 years versus aged <70 years by χ^2 test. [c] Women aged ≥70 years versus women aged <70 years by χ^2 test. [d] Men aged ≥70 years versus men aged <70 years by χ^2 test.

ible ('poor', 'fair' or 'good'), whereas TBWs with 'invisible' MB or LSW could not gain any contrast improvement for M1 detection.

TCCS is widely used to evaluate the intracranial arterial system in patients with acute stroke. The main limitation of TCCS arises from poor acoustic insonation conditions via the TBW, particularly in Asians, women and older patients. The failure rate because of an insufficient acoustic bone window is approximately 10–20% of patients in Western countries [8–10] and 20–30% of

Table 2. Anterior (ACA) and posterior cerebral artery (segment 1 and 2) detectabilities of 77 TBWs with 'INVISIBLE' M1

	INVISIBLE	POOR	FAIR	GOOD
ACA	73	3	1	0
P1	71	5	1	0
Proximal P2	59	10	6	2
Distal P2	57	4	11	5

Values are represented by numbers of TBWs.

Table 3. Relationship between structural visualization and M1 detectability

		M1 detectability				Spearman's ρ	p
		INVISIBLE	POOR	FAIR	GOOD		
CTB	invisible (3 TBWs)	3	0	0	0	0.68	<0.0001
	poor (34 TBWs)	33	0	1	0		
	fair (54 TBWs)	32	8	4	10		
	good (61 TBWs)	9	3	6	43		
MB	invisible (55 TBWs)	48	5	1	1	0.66	<0.0001
	poor (36 TBWs)	19	3	4	10		
	fair (39 TBWs)	7	2	5	25		
	good (22 TBWs)	3	1	1	17		
LSW	invisible (25 TBWs)	25	0	0	0	0.80	<0.0001
	poor (34 TBWs)	31	2	1	0		
	fair (44 TBWs)	20	6	5	13		
	good (49 TBWs)	1	3	5	40		

Values are represented by numbers of TBWs.

patients in Asian countries [4, 5]. In our study, this rate was 51%. Low M1 detectability in women and older patients was consistent with previous reports [9, 10]. Therefore, simple indicators to judge acoustic insonation conditions via the TBW are important to evaluate the M1 segment.

Insonations of B mode and color Doppler seem to be similarly affected by the temporal bone, because structural visibilities on B-mode images had significantly positive correlations with M1 detectability on color Doppler images for all patients, by sex and by age. The closer spatial relationship of the M1 with the LSW than with the CTB or MB seems to explain the present results that LSW visibility had the best correlation with M1 detectability. When the M1 was 'INVISIBLE' on color Doppler images, the precommunicating segment, proximal and distal postcommunicating segments were detected in 32% but the anterior cerebral artery was rarely detectable via the same TBW. Based on our results, the following criteria for

Table 4. M1 detectability improvement by contrast enhancement

		Improvement of M1 detectability
CTB	invisible (0 TBWs)	–
	poor (4 TBWs)	0
	fair (5 TBWs)	1 (20)
	good (11 TBWs)	7 (64)
MB	invisible (6 TBWs)	0
	poor (7 TBWs)	4 (57)
	fair (4 TBWs)	3 (75)
	good (3 TBWs)	1 (33)
LSW	invisible (5 TBWs)	0
	poor (6 TBWs)	3 (50)
	fair (7 TBWs)	4 (57)
	good (2 TBWs)	1 (50)

Values are represented by numbers of TBWs, with percentages in parentheses.

M1 evaluation on TCCS were developed. If the LSW is almost totally visible, M1 occlusion may be considered in patients with M1 invisibility. If the LSW is invisible or less than 50% visible, M1 invisibility on TCCS does not directly indicate M1 occlusion, and an additional imaging modality, such as MRA or CT angiography, is required. If the LSW is more than 50% visible and the M1 is not detectable, more than 50% or totally, visibility of the CTB and MB indicates probable M1 occlusion.

The addition of an ultrasound contrast agent allows adequate diagnosis in about 80–90% of patients with insufficient bone windows [12–20]. In our Japanese stroke patients, 40% of TBWs had an improved detection of the M1 on contrast-enhanced examination. In patients with invisible structures on B mode images, the administration of a contrast agent did not result in vessel identification. Therefore, TBWs with poor, fair and good visibility and insufficient M1 detection seem to be appropriate candidates for contrast-enhanced TCCS examination.

There were some limitations in this study. First, M1 occlusion on TCCS cannot be discussed from our findings because of the study exclusion of patients with luminal stenosis >50% or occlusion of the M1 or ICA on MRA and those with large infarction which may cause brain displacement. Second, severe atherosclerosis often causes arterial tortuosity and calcification. Arterial tortuosity might shift the M1 further from the LSW, and calcification might prevent ultrasound insonation. Third, machine specificity might affect structural visibility and M1 detectability. Fourth, the small sample size might affect the statistical correlation between the M1 detectability and the visibility of each anatomical structure, and a larger study might be needed to confirm our results. Finally, because our vascular neurologists knew that all the patients had a patent M1, the results might be overestimated.

Conclusion

The visibility of the LSW on B mode images was well correlated with M1 detection in Japanese aged patients with acute ischemic stroke having a patent M1. Our findings warrant future studies to determine detailed criteria of M1 occlusion using TCCS in patients with acute ischemic stroke.

Acknowledgments

This study was supported in part by a Grant-in-Aid (H21-Trans-Ippan-008) from the Ministry of Health, Labor and Welfare of Japan, and a grant from the Japan Cardiovascular Research Foundation (the Bayer Scholarship for Cardiovascular Research).

Disclosure Statement

None.

References

1 Hou WH, Liu X, Duan YY, Wang J, Sun SG, Deng JP, Qin HZ, Cao TS: Evaluation of transcranial color-coded duplex sonography for cerebral artery stenosis or occlusion. Cerebrovasc Dis 2009;27:479–484.

2 Malferrari G, Bertolino C, Casoni F, Zini A, Sarra VM, Sanguigni S, Pratesi M, Lochner P, Coppo L, Brusa G, Guidetti D, Cavuto S, Marcello N: The eligible study: ultrasound assessment in acute ischemic stroke within 3 hours. Cerebrovasc Dis 2007;24:469–476.

3 Baumgartner RW: Transcranial color duplex sonography in cerebrovascular disease: a systematic review. Cerebrovasc Dis 2003;16: 4–13.

4 Nedelmann M, Stolz E, Gerriets T, Baumgartner RW, Malferrari G, Seidel G, Kaps M: Consensus recommendations for transcranial color-coded duplex sonography for the assessment of intracranial arteries in clinical trials on acute stroke. Stroke 2009;40:3238–3244.

5 Seidel G, Kaps M, Gerriets T: Potential and limitations of transcranial color-coded sonography in stroke patients. Stroke 1995;26: 2061–2066.

6 Kenton AR, Martin PJ, Abbott RJ, Moody AR: Comparison of transcranial color-coded sonography and magnetic resonance angiography in acute stroke. Stroke 1997;28: 1601–1606.

7 Krejza J, Swiat M, Pawlak MA, Oszkinis G, Weigele J, Hurst RW, Kasner S: Suitability of temporal bone acoustic window: Conventional TCD versus transcranial color-coded duplex sonography. J Neuroimaging 2007;17: 311–314.

8 Halsey JH: Effect of emitted power on waveform intensity in transcranial Doppler. Stroke 1990;21:1573–1578.

9 Itoh T, Matsumoto M, Handa N, Maeda H, Hougaku H, Hashimoto H, Etani H, Tsukamoto Y, Kamada T: Rate of successful recording of blood flow signals in the middle cerebral artery using transcranial Doppler sonography. Stroke 1993;24:1192–1195.

10 Yagita Y, Etani H, Handa N, Itoh T, Imuta N, Okamoto M, Matsumoto M, Kinoshita N, Nukada T: Effect of transcranial Doppler intensity on successful recording in Japanese patients. Ultrasound Med Biol 1996;22:701–705.

11 Krejza J, Mariak Z, Melhem ER, Bert RJ: A guide to the identification of major cerebral arteries with transcranial color Doppler sonography. AJR 2000;174:1297–1303.

12 Zunker P, Wilms H, Brossmann J, Georgiadis D, Weber S, Deuschl G: Echo contrast-enhanced transcranial ultrasound: frequency of use, diagnostic benefit, and validity of results compared with MRA. Stroke 2002;33: 2600–2603.

13 Postert T, Braun B, Meves S, Koster O, Przuntek H, Weber S, Buttner T: Contrast-enhanced transcranial color-coded sonography in acute hemispheric brain infarction. Stroke 1999;30:1819–1826.
14 Gerriets T, Seidel G, Fiss I, Modrau B, Kaps M: Contrast-enhanced transcranial color-coded duplex sonography: efficiency and validity. Neurology 1999;52:1133–1137.
15 Baumgartner RW, Arnold M, Gonner F, Staikow I, Herrmann C, Rivoir A, Muri RM: Contrast-enhanced transcranial color-coded duplex sonography in ischemic cerebrovascular disease. Stroke 1997;28:2473–2478.
16 Bogdahn U, Becker G, Schlief R, Reddig J, Hassel W: Contrast-enhanced transcranial color-coded real-time sonography. Results of a phase-two study. Stroke 1993;24:676–684.
17 Goertler M, Kross R, Baeumer M, Jost S, Grote R, Weber S, Wallesch CW: Diagnostic impact and prognostic relevance of early contrast-enhanced transcranial color-coded duplex sonography in acute stroke. Stroke 1998;29:955–962.
18 Nabavi DG, Droste DW, Kemeny V, Schulte-Altedorneburg G, Weber S, Ringelstein EB: Potential and limitations of echocontrast-enhanced ultrasonography in acute stroke patients: a pilot study. Stroke 1998;29:949–954.
19 Kunz A, Hahn G, Mucha D, Muller A, Barrett KM, von Kummer R, Gahn G: Echo-enhanced transcranial color-coded duplex sonography in the diagnosis of cerebrovascular events: a validation study. AJNR Am J Neuroradiol 2006;27:2122–2127.
20 Seidel G, Meairs S: Ultrasound contrast agents in ischemic stroke. Cerebrovasc Dis 2009;27(suppl 2):25–39.

Original Paper

Cerebrovascular Diseases

Cerebrovasc Dis 2012;33:369–377
DOI: 10.1159/000336121

Received: March 22, 2011
Accepted: December 21, 2011
Published online: March 14, 2012

Identification of Internal Carotid Artery Dissection by Transoral Carotid Ultrasonography

Rieko Suzuki[a] Masatoshi Koga[b] Kazunori Toyoda[a] Masahiro Uemura[c]
Hikaru Nagasawa[a] Yusuke Yakushiji[a] Hiroshi Moriwaki[c] Naoaki Yamada[d]
Kazuo Minematsu[a]

[a]Department of Cerebrovascular Medicine, [b]Division of Stroke Care, [c]Department of Neurology, and
[d]Department of Radiology, National Cerebral and Cardiovascular Center, Suita, Japan

Key Words
Transoral carotid ultrasonography · Cerebrovascular disease · Internal carotid artery dissection · Stroke

Abstract
Background and Purpose: Conventional transsurface carotid ultrasonography (TSCU) via the cervical surface often fails to detect dissection of the extracranial internal carotid artery (ICA). The role of transoral carotid ultrasonography (TOCU) in the detection of ICA dissection was examined. ***Method:*** Patients with unilateral extracranial ICA dissection identified by digital subtraction angiography (DSA) from our database of patients with ischemic stroke or transient ischemic attack (TIA) were reviewed. Findings of dissection were compared between TSCU and TOCU. ***Results:*** Eight patients (7 men, 37–69 years old), including 7 with ischemic stroke and 1 with TIA, had ICA dissection. By DSA, dissection was identified between the first and third vertebrae in 4 patients and from the third cervical vertebra to the intracranial level in the remaining 4. TOCU images revealed an intimal flap as definite evidence of dissection in all patients. In 7 patients, color flow signals were not seen in false lumens, indicating thrombosed lumens. Four patients showed morphological changes of dissection on follow-up TOCU, including a patient with recovery of color flow signals in false lumens. The diameter of the dissected ICA was 7.3 ± 0.7 mm and that of the contralateral ICA was 4.9 ± 0.6 mm ($p = 0.008$). In contrast, TSCU did not enable any conclusive findings of ICA dissection to be made in any patient. Six patients had intramural hematoma on T_1-weighted MRI, and 2 had an intimal flap with a double lumen on magnetic resonance angiography. ***Conclusion:*** TOCU has advantages over TSCU in achieving an accurate diagnosis and follow-up evaluation of ICA dissection.

Introduction

Internal carotid arterial (ICA) dissection accounts for approximately 2–3% of all ischemic strokes [1, 2] and is one of the important causes of stroke in young and middle-aged patients [3–6]. The pathogenesis of ICA dissection is often unknown. Most ICA dissections occur spontaneously or follow a sudden head movement, a chiropractic manipulation, and many types of sports activities [7, 8]. Because ICA dissection sometimes causes brain ischemia and subarachnoid hemorrhage [6], immediate vascular evaluation and treatment are necessary. Among the diagnostic tools for identifying dissections, including

KARGER
Fax +41 61 306 12 34
E-Mail karger@karger.ch
www.karger.com

1015–9770/12/0334–0369$38.00/0

Accessible online at:
www.karger.com/ced

Masatoshi Koga, MD
Division of Stroke Care
National Cerebral and Cardiovascular Center
5-7-1 Fujishirodai, Suita, Osaka 565-8565 (Japan)
Tel. +81 6 6833 5012, E-Mail koga@hsp.ncvc.go.jp

digital subtraction angiography (DSA) [9, 10], magnetic resonance imaging (MRI) [11], magnetic resonance angiography (MRA) [12, 13], computed tomography angiography (CTA) [14–16] and conventional transsurface carotid ultrasonography (TSCU) [17–20], TSCU is handy and safe. However, ICA dissection typically occurs at least 2 cm distal to the bifurcation, at the level of the second and third cervical vertebrae, and extends over a variable distance [3]. The distal extracranial ICA cannot be examined by TSCU as it lies behind bones and cannot be imaged in B-mode. Doppler on TSCU can provide information about the distal ICA only if there is a flow-limiting stenosis or occlusion that results in abnormal waveforms. Thus, the lesion may be underdiagnosed by routine TSCU examination.

Transoral carotid ultrasonography (TOCU), a new ultrasound technique that was developed in our institute [21], can identify the distal extracranial ICA that is invisible on TSCU [21]. We and others have reported the utility of TOCU in evaluating various ICA pathologies, including distal extracranial ICA stenosis, occlusion, pseudo-occlusion, moya moya disease and dissection [22–28]. In particular, TOCU seems to be superior to TSCU in detecting ICA dissection during acute stroke because of its ability to visualize the high portion of the extracranial ICA. We previously reported some cases with ICA dissection proven by TOCU [26–28]. However, the utility of TOCU should be assessed not only in isolated cases. In this study, the utility of TOCU in evaluating consecutive patients with ICA dissection as the final diagnosis was examined based on comparison with other imaging modalities, such as DSA, MRI and TSCU.

Subjects and Methods

Patients with stroke or transient ischemic attack (TIA) caused by extracranial ICA dissection confirmed by DSA from our database of 6,026 patients with ischemic stroke or TIA who were admitted to our hospital between 1999 and 2010 were reviewed.

Basically, all patients in our database underwent intracranial MRI/MRA and TSCU unless MRI was contraindicated. When ICA stenosis or occlusion was detected on these regular examinations or when dissection was suspected as a cause of ICA lesions based on typical histories and symptoms, including sports activities and cephalocervical pain, or absence of other obvious causes for the lesions, DSA was performed after obtaining the patient's informed consent. Three-dimensional (3D) rotational angiography with a standard Integris BV5000 biplane system (Philips Medical System, Best, The Netherlands) was also performed if needed. The system provides contrast angiographic vascular luminal rotational X-ray image acquisition in multiple planes with reconstruction on a 3D work station [10]. The diagnosis of ICA dissection was made by DSA based on the review by Provenzale [11] and the criteria of the Spontaneous Cervicocephalic Arterial Dissections Study [29]. Briefly, the presence of an intimal flap with a double lumen was a direct finding for identifying ICA dissection. The pearl-and-string sign, string sign, pearl sign, retention of contrast, total occlusion with proximal distension, and tapered occlusion on DSA needed further evidence, such as morphological change on DSA or intramural hematoma on T_1 MRI. The level of the dissection was established based on DSA findings. The findings of TSCU, TOCU and MRI/MRA were compared using DSA as the gold standard. Patients' clinical backgrounds, stroke types, stroke risk factors, and prognoses were reviewed as well.

TSCU and TOCU Examinations

TSCU and TOCU examinations were performed using an ATL Ultramark 9 HDI (Advanced Technology Laboratories, Bothell, Wash., USA) with a 5- to 10-MHz linear probe and a 5- to 9-MHz micro convex probe, respectively, or an Aplio™ XU (Toshiba Co. Ltd, Tokyo, Japan) with a 7.5-MHz linear probe and a 6-MHz micro convex probe, respectively. For TSCU examination, the standard approach using B mode, color flow imaging, and pulsed Doppler was performed in the decubitus position. The probes for TOCU examination were originally designed for transrectal use. We performed TOCU in patients with ICA territory stroke who were suspected to have pathological lesions at the extracranial distal ICA based on TSCU or intracranial MRI/MRA findings; evaluation of the extracranial distal ICA was mandatory. We used a protocol for identifying patients who needed to undergo further evaluations for ICA dissection, notably patients with ICA territory ischemia or retinal ischemia of unknown etiology based on standard evaluations including head computed tomography, head MRI and MRA, TSCU, electrocardiogram monitoring and blood test. Those with concomitant symptoms or signs, such as headache, neck pain, face pain, ipsilateral Horner's syndrome, pulsatile tinnitus or lower cranial nerve palsy, were especially suspected of having ICA dissection. For such patients, DSA or cervical MRI/MRA was preferentially performed and TOCU was added if needed prior to mid-2008. After mid-2008, TOCU was preferentially performed. TOCU was repeated to evaluate morphological changes every 1–3 days during hospitalization when ICA dissection was detected on initial examination. The details of the TOCU examination procedure have been reported previously [21]. Briefly, the probe was covered with a disposable probe cover made of sterile thin gum after covering the tip of the probe with echo jelly. Then, the probe was inserted transorally and touched the pharyngeal posterolateral wall. Basically, we did not use local anesthesia because the pharyngeal reflex rarely occurs. For patients with severe pharyngeal reflex, one or two pushes of 8% xylocaine spray to the pharyngeal posterolateral wall were used. The display was in the vertical plane to longitudinally detect and assess extracranial ICA, and in the axial plane for horizontal assessment. The ICA was identified by delineation of a vessel running linearly from the lower to the upper pharynx and by confirming that flow was proceeding upward to the skull base and that branching was absent using B-mode and color flow imaging. The ICA was usually identified at the level of the second and third cervical vertebrae, based on our unpublished data, which show the spatial relationship between the TOCU probe and the cervical vertebrae on the X-ray. B-mode was used

Table 1. Clinical characteristics

	Case 1 [26]	Case 2 [28]	Case 3	Case 4 [27]	Case 5	Case 6	Case 7	Case 8
Sex	male	male	female	male	male	male	male	male
Age, years	37	52	62	69	51	57	42	48
Type of stroke	IS	TIA	IS	IS	IS	IS	IS	IS
Prior history of stroke	absent	absent	absent	absent	absent	absent	absent	absent
Risk factors	dyslipidemia, smoking, drinking	hypertension	none	none	none	none	hypertension	none
Affected side	right	right	right	left	right	left	right	left
Cephalocervical pain	headache	absent	absent	orbital pain	absent	absent	headache	headache
Neurological findings	hoarseness, hemiparesis	hemiparesis	dysarthria, hemiparesis	hyperesthesia, visual field blurring	USN, dysarthria, hemiparesis, hypoesthesia	aphasia	USN, dysarthria, hemiparesis, hypoesthesia	aphasia, hemiparesis

IS = Ischemic stroke; USN = unilateral spatial neglect.

to measure the distal ICA diameter from the near to the far adventitial edge. Pulsed Doppler was used to measure the flow velocity of the distal ICA with an angle correction within 60° between the blood flow direction and the Doppler interrogation. Color Doppler was used to identify flow signals in true and false lumens. The lumen which tapered from the ICA was defined as a true lumen and the other was defined as a false lumen [17]. When flow signals were absent in false lumens, the lumens were considered to be thrombosed. An intimal flap with a double lumen was a definite finding for identifying ICA dissection by both TSCU and TOCU. Furthermore, the maximum diameter of the dilated extracranial ICA was measured from the near to the far adventitial edges and compared with the diameter of the contralateral ICA at almost the same distance from the carotid bifurcation. The probe was carefully horizontally swept in the vertical plane to detect the maximum diameter of the vessel's center to avoid overmeasurement in case the vessel is tortuous or turning.

MR Examinations

MRI of the cervical ICA was performed on a 1.5-tesla scanner (Magnetom Vision or MAGNETOM Sonata, Siemens Medical Systems, Erlangen, Germany) with standard neck array coils. The MRI protocol was composed of T_1-weighted images and 3D-time of flight MRA. MRA was performed on both intracranial and extracranial vessels. Intracranial MRA was performed on admission and extracranial MRA was performed during hospitalization. Gadolinium-enhanced MRA was not performed routinely. Intramural hematoma and luminal diameter on both sides were assessed by T_1 MRI while intimal flap with double lumen, stenosis and dilatation, and pseudoaneurysm were evaluated by MRA by an experienced radiologist. Patients who did not tolerate MRI because of claustrophobia or because they had pacemakers were diagnosed based on brain CT and DSA.

Data Evaluation

Continuous variables were compared with the Wilcoxon signed rank test. A value of $p < 0.05$ was considered statistically significant.

Results

Eight patients (7 men, age 37–69 years) with extracranial ICA dissection were identified from the database. Seven patients developed ischemic stroke and 1 developed TIA ipsilaterally to the affected ICA. The initial TOCU examination was performed after confirmation of dissection by DSA in 5 patients and prior to DSA in the other 3 (cases 5, 6, 8), whose clinical history strongly suggested ICA dissection. The detailed clinical presentations of 3 of these 8 patients have been previously reported [26–28]. Table 1 summarizes the patients' clinical characteristics, and table 2 shows the results of the DSA, TSCU, TOCU and MRI/MRA examinations. The basis of the diagnosis by DSA was the double-lumen sign with an intimal flap in 2, dilatation and stenosis in 3, and tapered occlusion in 4. On DSA, the dissection site was restricted to the level between the first and third cervical vertebrae in 4 patients, and the dissection extended from the third cervical vertebra to the intracranial ICA in the remaining 4 patients. Four patients showed morphological changes of dissection on follow-up DSA. In case 2, who initially had an intimal flap with a double lumen on day 1, a saccular type pseudoaneurysm was detected on day 16. In case 4, who initially had severe stenosis on day 1, an intimal flap with a double lumen with a fusiform-type pseudoaneurysm appeared on day 7. In case 5, who initially had proximal dilatation and stenosis, and a distal saccular-type aneurysm on day 3, the stenotic lesion became wider and an additional aneurysm was detected on day 19. In case 8, who initially had an ICA tapering occlusion on day 1, the ICA was recanalized on day 17. Figures 1 and

Table 2. Imaging findings

Modality	Findings	Case 1 [26]	Case 2 [28]	Case 3	Case 4 [27]	Case 5	Case 6	Case 7	Case 8
CT/MRI	location of ischemia	ant-choroid, PCA	corona radiata	MCA cortex	MCA central gyrus	MCA cortex and deep area	MCA cortex	MCA cortex	MCA cortex
DSA	location of dissection	C3-siphon	C1–C2	C1–C2	C1–C2	C1–C3	C3-distal IC	C3-distal IC	C3-distal IC
	location of carotid artery bifurcation	between C3 and C4	C3	between C3 and C4	C3	between C3 and C4	C4	C4	between C3 and C4
	intimal flap with double lumen[1]	–	–	present	present	–	–	–	–
	dilatation and stenosis	–	present	–	present	present	–	–	–
	tapering occlusion	present	–	–	–	–	present	present	present
	pseudoaneurysm	–	saccular	fusiform	fusiform	saccular	–	–	–
	morphological change	–	present	–	present	present	–	–	present
TOCU	intimal flap/double lumen[1]	present	present	present	present	present	present	present	present
	false lumen	thrombosed	thrombosed	not thrombosed	thrombosed[2]	thrombosed	thrombosed	thrombosed	thrombosed[2]
	stenosis	–	present	–	present	present	–	–	–
	occlusion	–	–	–	–	–	–	–	–
	dissected arterial diameter, mm	7.1	7.3	6.3	7.0	7.9	6.5	7.7	6.5
	contralateral arterial diameter, mm	5.0	4.0	5.6	5.6	4.4	4.9	4.2	4.9
	pseudoaneurysm	–	undetectable	fusiform	fusiform	saccular	–	–	–
	morphological change	–	present	–	present	present	–	–	present
	initial Doppler flow abnormality	present[3]	present[4]	–	present[3]	–	present[3]	present[3]	present[3]
	sequential flow pattern change	–	present[2]	–	present[4]	present[4]	–	–	present[5]
TSCU	intimal flap/double lumen[1]	–	–	–	–	–	–	–	–
	arterial narrowing	present	–	–	–	present	–	–	present
	dissected arterial diameter, mm	8.8	9.9	4.3	6.7	5.8	4.5	4.8	8.5
	contralateral arterial diameter, mm	7.3	5.9	4.0	5.3	6.0	4.8	4.3	5.4
	arterial dilatation	–	present	–	–	–	–	–	–
	morphological change	–	–	–	–	present	–	–	present
	initial Doppler flow abnormality	present[3]	–	–	present[3]	–	present[3]	present[3]	present[3]
	sequential flow pattern change	–	–	–	present[5]	present[4]	–	–	present[5]
Cervical MRI and MRA	intimal flap with double lumen	–	–	present	present	–	–	–	–
	intramural hematoma	present	present	–	–	present	present	present	present
	ICA stenosis	–	present	–	–	present	–	–	present
	occlusion	present	–	–	–	–	present	present	present
	pseudoaneurysm	–	present	–	–	present	–	–	–

ant-choroid = Anterior choroidal artery; C1 = first cervical vertebra level; C2 = second cervical vertebra level; C3 = third cervical vertebra level; CT = computed tomography; MCA = middle cerebral artery; PCA = posterior cerebral artery; siphon, carotid siphon; USN = unilateral spatial neglect; C1–3 = cervical vertebra levels; siphon, carotid siphon.

[1] Direct findings of arterial dissection.

[2] Normalized peak flow velocity.

[3] Absence of end diastolic velocity indicating distal occlusion.

[4] High peak flow velocity (>200 cm/s) indicating stenosis.

[5] Normalized end-diastolic flow velocity.

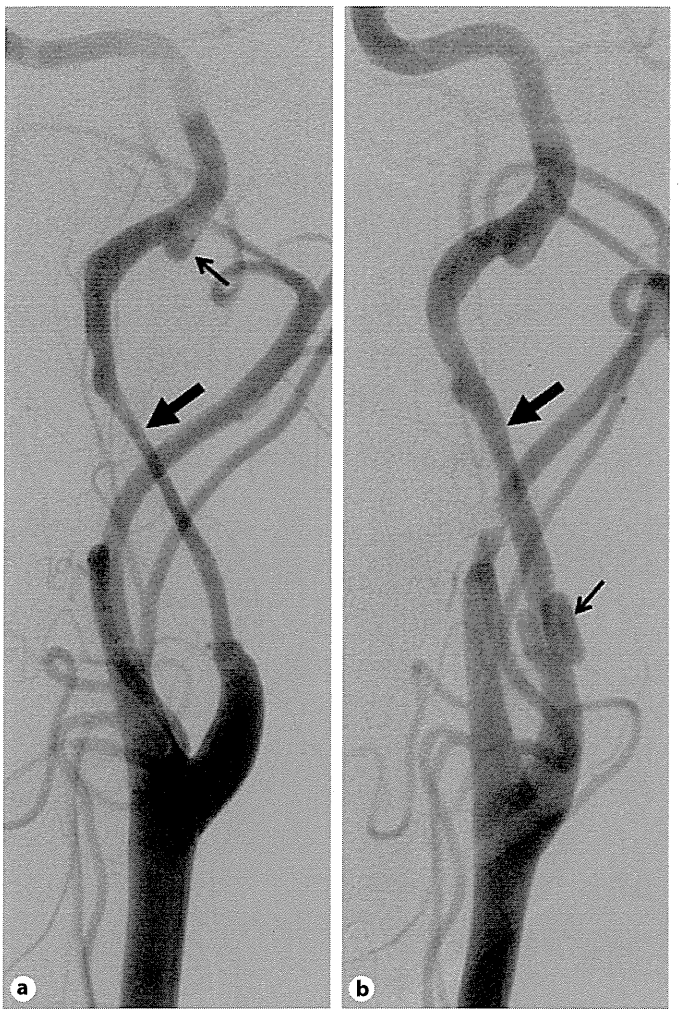

Fig. 1. Dissection of the extracranial ICA on a common carotid DSA image in case 5. **a** Right anterior oblique view on day 3. Dilatation and stenosis in the proximal ICA (thick arrow) and an aneurysm in the distal extracranial ICA (thin arrow) are shown. **b** Right anterior oblique view on day 19. The stenotic lesion becomes wider (thick arrow). A new aneurysm appears in the proximal ICA (thin arrow).

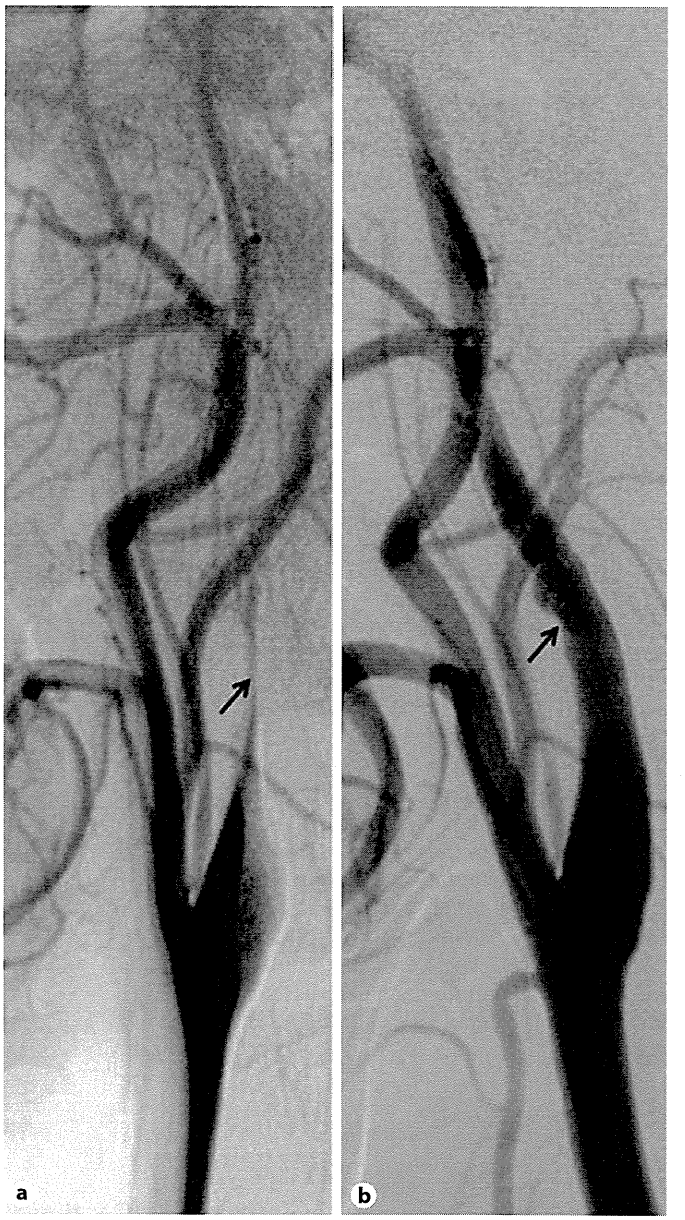

Fig. 2. Dissected ICA on a common carotid DSA image in case 8. **a** Lateral view on day 1, showing tapering ICA occlusion (arrow). **b** Recanalized dissected ICA (arrow) on day 17.

2 show sequential DSA images in cases 5 and 8, respectively.

By TOCU, a double lumen with an intimal flap was identified in all 8 patients. Color signals were absent in false lumens of 7 patients on the initial TOCU, indicating a thrombosed lumen; on the 2nd follow-up TOCU, little forward blood flow was present in the false lumen and in the course of time the flow volume increased gradually, indicating disappearance of the intraluminal thrombi in 1 patient (case 4) [27]. The luminal diameter at the height of the second cervical vertebra was 7.3 ± 0.7 mm in the dissected ICA and 4.9 ± 0.6 mm in the contralateral ICA in all patients ($p = 0.008$). No patient had a tortuous or turning vessel at the measurement point. On the initial Doppler examination, 5 patients displayed absence of end-diastolic velocity, indicating distal ICA occlusion, and 1 patient had ICA stenosis. As all the occluded arte-

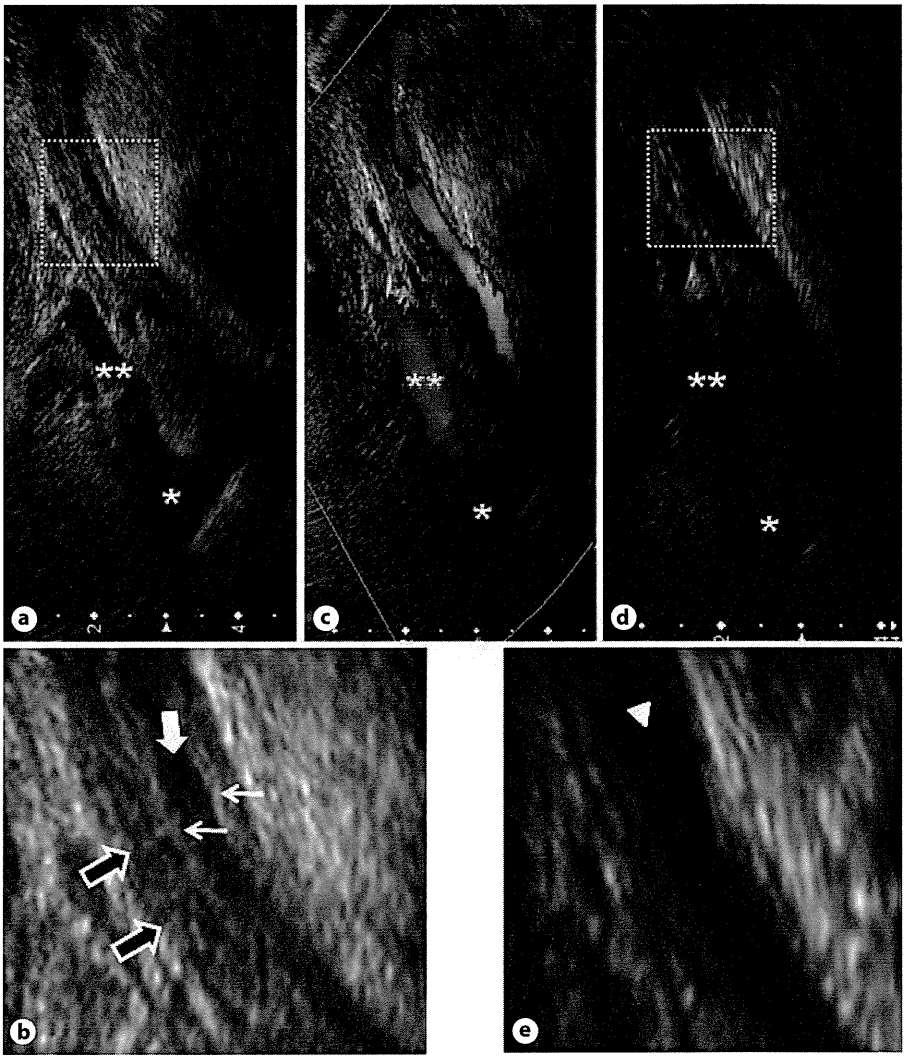

Fig. 3. Dissected ICA on TOCU images in case 5. **a**, **b** Longitudinal B-mode image of the right ICA on day 3. Narrowing of the true lumen (thick arrow), thrombosed false lumens (open arrows), and intimal flaps (thin arrows) are shown more than 2 cm distal to the carotid bifurcation. **c** Color Doppler image on day 3. Antegrade blood flow in the true lumen is observed. **d**, **e** Follow-up B-mode images on day 26. The true lumen turns wider (arrowhead). * and ** indicate the carotid bifurcation and external carotid artery, respectively. **b**, **e** Magnified images of lesions surrounded by dotted frames in **a** and **d**, respectively.

rial sites were at the level of the intracranial ICA, direct findings of ICA occlusion were not made by TOCU. On follow-up TOCU, dynamic changes of the dissected artery were detected in 4 patients (cases 2, 4, 5, 8). Narrowing of the true lumen and increased flow velocity, indicating a stenotic change in the ICA, improved on sequential follow-up TOCU (cases 2, 4, 5). In case 8, reperfusion with antegrade blood flow of the true lumen was detected. A pseudoaneurysm was detected in 3 patients (cases 3–5), and a pseudoaneurysm was missed in case 2, probably due to its high position. Figures 3 and 4 show sequential TOCU images in cases 5 and 8, respectively.

In contrast, definite findings specific to dissections, including a double lumen with an intimal flap, could not be made by TSCU in any patients. Six patients (cases 1, 4–8) showed nonspecific findings indicative of arterial stenosis or occlusion; 3 had mild arterial narrowing (<50%) with presumably a thin, echogenic intravascular structure which probably represents an intimal flap was found at a short distance above the bifurcation on B-mode images [17], 5 (cases 1, 4, 6, 7, 8) had absent end-diastolic flow of the ICA, suggesting distal ICA occlusion, and 1 (case 5) had increased peak systolic flow velocity exceeding 200 cm/s (203 cm/s), suggesting ICA stenosis.

Arterial dilatation of the proximal carotid ICA was visualized in only 2 patients by TSCU whereas TOCU identified arterial dilatation of the dissected extracranial ICA using in all patients.

Cervical MRI/MRA was performed in all patients from 6 days to 1 month after stroke onset. Gadolinium-

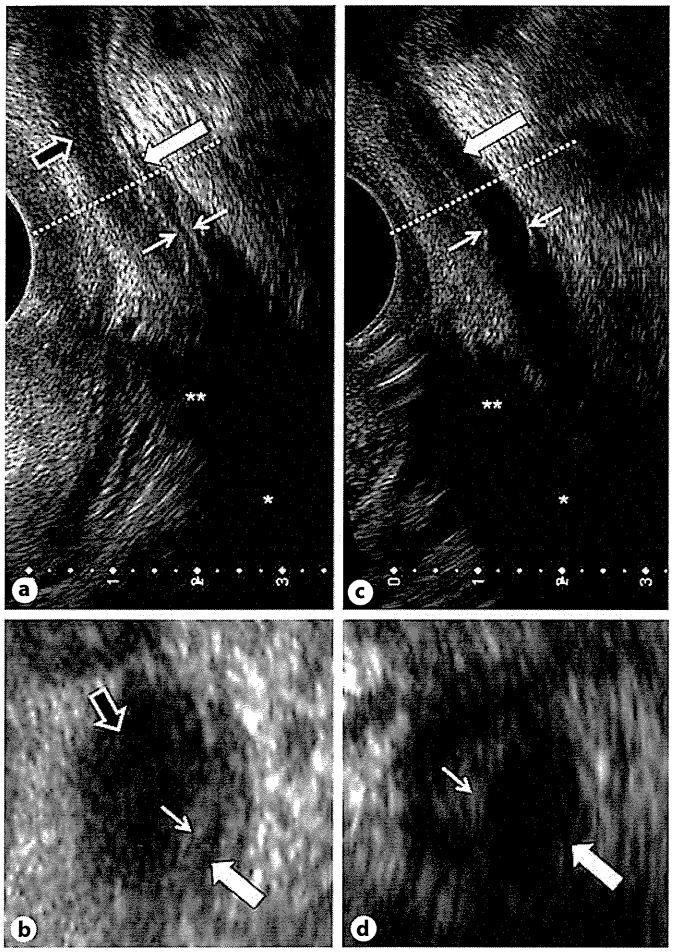

Fig. 4. Dissected ICA on TOCU images in case 8. **a**, **b** Longitudinal (**a**) and axial (**b**) B-mode TOCU images on day 8, showing narrowing of the true lumen (filled arrows), thrombosed false lumens (open arrows), and intimal flaps (thin arrows). **c**, **d** Follow-up B-mode images on day 32. The wider true lumen (filled arrows) and intimal flaps (thin arrows) are shown. * and ** indicate the carotid bifurcation and external carotid artery, respectively. Dotted lines in **a** and **c** indicate the levels of axial B-mode in **b** and **d**, respectively.

enhanced MRA was performed in 3 patients (cases 2, 5, 6). Cervical MRA images revealed an intimal flap with a double lumen in 2 patients, ICA stenosis and a pseudoaneurysm in another 2 patients, and ICA tapering occlusion and a thrombosed false lumen in 4 patients. On the axial view of T_1-weighted MRI, 6 patients had intramural hematomas, with high signals between the first and third cervical vertebrae in 2 and from the third vertebra to the intracranial ICA in 4. The luminal diameter on T_1-weighted images was 7.7 ± 0.9 mm in the dissected ICA and 5.6 ± 0.8 mm in the contralateral ICA ($p = 0.008$).

Discussion

The utility of TOCU in the diagnosis of ICA dissection has only been reported in isolated case reports, all from our institute [26–28]. This is the first report on the identification of ICA dissection using TOCU in consecutive stroke patients with ICA dissection as the final diagnosis. The first major finding of this study is that TOCU provided results comparable with those made by DSA and MRA for the diagnosis of dissection based on the presence of an intimal flap with a double lumen in all patients. Although Benninger et al. [30] reported that TSCU plus transcranial ultrasound was highly accurate in the diagnosis of ICA dissection, their definition of the diagnosis was mainly based on indirect findings, such as changes in the ICA blood flow pattern. It seems to be difficult to identify direct findings such as intimal flap and double lumens by TSCU. In addition, several unique signs, such as arterial stenosis, patency and thrombotic changes in true and false lumens, were also easily detectable using TOCU. The second major finding is that sequential changes in morphology and color flow signals, which are other important findings indicative of dissection, were identified in half of the present patients on follow-up TOCU. Third, a larger luminal diameter of the dissected ICA as compared with the contralateral ICA was measurable by TOCU. These results show the advantages of TOCU over TSCU in the diagnosis of dissection. Since the carotid artery bifurcation is generally higher in Asian patients (at the lower part of the third cervical vertebra) than in Western patients (approximately the fourth cervical vertebra) [31, 32], TOCU seems to be especially useful in Asian patients.

The utility of TOCU in the diagnosis of ICA dissections has changed over the last 12 years. In 5 of 8 patients in whom ICA dissections had already been proven by DSA, TOCU was simply used to confirm the diagnosis and to follow up changes over time. In 3 recent patients, we used TOCU before DSA in those with suspected ICA dissection whereas we preferred cervical MRI/MRA evaluations for suspected lesions of the extracranial distal ICA.

Since TOCU was not done in all of the patients of our database, the specificity of the diagnosis of ICA dissection using TOCU cannot be assessed. Thus, we cannot conclude that TOCU represents a gold standard for diagnosing dissections. At least, one can say that TOCU is useful for identifying false lumens and obtaining information as to their blood flow. For example, changes in the color flow signals in the false lumen indicate growth or

decrease of intramural clots. In contrast, DSA often delineates false lumens as nonspecific arterial stenosis or occlusion and requires a 3D rotational technique for detailed identification. T_1-weighted MRI of an intramural hematoma is better or more convincing, especially in cases of ICA occlusion identified by DSA. TOCU is superior to MRI and MRA for the documentation of real-time blood flow visualization and flow velocity measurement; such information reflects changes in arterial diameter and arterial reopening. In patients with only flap and/or aneurysmal dilatation TOCU might provide complementary information to that provided by DSA and MRI/MRA. In addition, TOCU is noninvasive, does not augment the dissection, and is easily repeatable at the bedside. Thus, TOCU is available both as a screening and as a frequent follow-up method of uncommon strokes. For example, a patient with developing arterial dilatation or aneurysmal change on follow-up within a short interval is a candidate for emergent surgery or intra-arterial catheter treatment.

The tip of the probe is about 2 cm across in diameter. The pharyngeal reflex rarely occurs because the probe just touches the posterolateral wall and the examination usually takes only a few minutes. Based on our unpublished data, ICA was visible without local anesthesia in more than 95% of the patients and no patients had aspiration pneumonia related to TOCU.

This study has some limitations. The first limitation is the small patient number, which partly results from the ethnic peculiarity; a nationwide survey in Japan indicates that only 2.4% of all patients with cervicocephalic dissection had extracranial ICA dissection whereas 63% had intracranial vertebral artery dissection [29]. Second, some patients having ICA dissection might have been misdiagnosed and might have missed the opportunity to undergo TOCU. DSA is not routine for all stroke inpatients and the lack of universally established criteria for dissection might prevent accurate diagnosis even by DSA. Third, TOCU was performed after DSA in the initial 5 patients; this caused sample selection bias. Finally, the imaging quality of TOCU has greatly improved during the 10-year study period; e.g. a newer Aplio™ XU with a 6-MHz micro convex probe provides a wider view of the ICA (up to 6–7 cm from the bifurcation) than the ATL Ultramark 9 HDI with a 5- to 9-MHz micro convex probe (approximately up to 3 cm) [21].

In conclusion, TOCU enabled definite diagnoses of extracranial ICA dissection and was superior to conventional TSCU. TOCU is a promising diagnostic tool in patients with extracranial ICA dissection.

Acknowledgments

This study was supported in part by a grant from the Japan Cardiovascular Research Foundation (the Bayer Scholarship for Cardiovascular Research) and by the Intramural Research Fund (23-6-4) for Cardiovascular Diseases of the National Cerebral and Cardiovascular Center.

Disclosure Statement

None.

References

1 Biller J, Hingtgen WL, Adams HP Jr, Smoker WR, Godersky JC, Toffol GJ: Cervicocephalic arterial dissections. A ten-year experience. Arch Neurol 1986;43:1234–1238.

2 Bogousslavsky J, Despland PA, Regli F: Spontaneous carotid dissection with acute stroke. Arch Neurol 1987;44:137–140.

3 Schievink WI, Mokri B, Piepgras DG: Spontaneous dissections of cervicocephalic arteries in childhood and adolescence. Neurology 1994;44:1607–1612.

4 Lee VH, Brown RD Jr, Mandrekar JN, Mokri B: Incidence and outcome of cervical artery dissection: a population-based study. Neurology 2006;67:1809–1812.

5 Arnold M, Kappeler L, Georgiadis D, Berthet K, Keserue B, Bousser MG, Baumgartner RW: Gender differences in spontaneous cervical artery dissection. Neurology 2006;67:1050–1052.

6 Touze E, Gauvrit JY, Moulin T, Meder JF, Bracard S, Mas JL: Risk of stroke and recurrent dissection after a cervical artery dissection: a multicenter study. Neurology 2003;61:1347–1351.

7 Lee KP, Carlini WG, McCormick GF, Albers GW: Neurologic complications following chiropractic manipulation: a survey of California neurologists. Neurology 1995;45:1213–1215.

8 Peters M, Bohl J, Thomke F, Kallen KJ, Mahlzahn K, Wandel E, Meyer zum Buschenfelde KH: Dissection of the internal carotid artery after chiropractic manipulation of the neck. Neurology 1995;45:2284–2286.

9 Pelkonen O, Tikkakoski T, Leinonen S, Pyhtinen J, Lepojarvi M, Sotaniemi K: Extracranial internal carotid and vertebral artery dissections: angiographic spectrum, course and prognosis. Neuroradiology 2003;45:71–77.

10 Matsumoto S, Takada T, Yasaka M, Kasuya J, Yamada K, Naritomi H, Minematsu K: Intracranial arterial dissections in ischemic stroke assessed by 3D rotational angiography. J Neurol Sci 2010;296:55–58.

11 Provenzale JM: Dissection of the internal carotid and vertebral arteries: imaging features. AJR Am J Roentgenol 1995;165:1099–1104.
12 Klufas RA, Hsu L, Barnes PD, Patel MR, Schwartz RB: Dissection of the carotid and vertebral arteries: imaging with MR angiography. AJR Am J Roentgenol 1995;164:673–677.
13 Nguyen Bui L, Brant-Zawadzki M, Verghese P, Gillan G: Magnetic resonance angiography of cervicocranial dissection. Stroke 1993;24:126–131.
14 Leclerc X, Godefroy O, Salhi A, Lucas C, Leys D, Pruvo JP: Helical CT for the diagnosis of extracranial internal carotid artery dissection. Stroke 1996;27:461–466.
15 Petro GR, Witwer GA, Cacayorin ED, Hodge CJ, Bredenberg CE, Jastremski MS, Kieffer SA: Spontaneous dissection of the cervical internal carotid artery: correlation of arteriography, CT, and pathology. AJR Am J Roentgenol 1987;148:393–398.
16 Zuber M, Meary E, Meder JF, Mas JL: Magnetic resonance imaging and dynamic CT scan in cervical artery dissections. Stroke 1994;25:576–581.
17 Steinke W, Rautenberg W, Schwartz A, Hennerici M: Noninvasive monitoring of internal carotid artery dissection. Stroke 1994; 25:998–1005.
18 Sturzenegger M, Mattle HP, Rivoir A, Baumgartner RW: Ultrasound findings in carotid artery dissection: analysis of 43 patients. Neurology 1995;45:691–698.
19 de Bray JM, Lhoste P, Dubas F, Emile J, Saumet JL: Ultrasonic features of extracranial carotid dissections: 47 cases studied by angiography. J Ultrasound Med 1994;13:659–664.
20 Mullges W, Ringelstein EB, Leibold M: Noninvasive diagnosis of internal carotid artery dissections. J Neurol Neurosurg Psychiatry 1992;55:98–104.
21 Yasaka M, Kimura K, Otsubo R, Isa K, Wada K, Nagatsuka K, Minematsu K, Yamaguchi T: Transoral carotid ultrasonography. Stroke 1998;29:1383–1388.
22 Yasaka M, Ogata T, Yasumori K, Inoue T, Okada Y: Bottle neck sign of the proximal portion of the internal carotid artery in moyamoya disease. J Ultrasound Med 2006;25: 1547–1552.
23 Fujimoto S, Toyoda K, Kishikawa K, Inoue T, Yasumori K, Ibayashi S, Iida M, Okada Y: Accuracy of conventional plus transoral carotid ultrasonography in distinguishing pseudo-occlusion from total occlusion of the internal carotid artery. Cerebrovasc Dis 2006;22: 170–176.
24 Isa K, Yasaka M, Kimura K, Nagatsuka K, Minematsu K: Transoral carotid ultrasonography for evaluating internal carotid artery occlusion. Intern Med 2005;44:567–571.
25 Kishikawa K, Kamouchi M, Okada Y, Inoue T, Ibayashi S, Iida M: Transoral carotid ultrasonography as a diagnostic aid in patients with severe carotid stenosis. Cerebrovasc Dis 2004;17:106–110.
26 Koga M, Kimura K, Minematsu K, Yasaka M, Isa K, Yamaguchi T: Transoral carotid ultrasonographic findings in internal carotid artery dissection – a case report. Angiology 2000;51:699–703.
27 Nagasawa H, Tomii Y, Yokota C, Toyoda K, Matsuoka H, Suzuki R, Minematsu K: Images in cardiovascular medicine. Acute morphological change in an extracranial carotid artery dissection on transoral carotid ultrasonography. Circulation 2008;118:1064–1065.
28 Yakushiji Y, Yasaka M, Takada T, Minematsu K: Serial transoral carotid ultrasonographic findings in extracranial internal carotid artery dissection. J Ultrasound Med 2005;24: 877–880.
29 Minematsu K, Matsuoka H, Kasuya J: Cervicocephalic arterial dissection in Japan: Analysis of 454 patients in the spontaneous cervicocephalic arterial dissection study 1 (SCADS-1) (abstract). Stroke 2008;566.
30 Benninger DH, Georgiadis D, Gandjour J, Baumgartner RW: Accuracy of color duplex ultrasound diagnosis of spontaneous carotid dissection causing ischemia. Stroke 2006;37: 377–381.
31 Hayashi N, Hori E, Ohtani Y, Ohtani O, Kuwayama N, Endo S: Surgical anatomy of the cervical carotid artery for carotid endarterectomy. Neurol Med Chir (Tokyo) 2005;45: 25–29; discussion 30.
32 Toyota A, Shima T, Nishida M, Yamane K, Okada Y, Csiba L, Kollar J, Sikula J: Angiographical evaluation of extracranial carotid artery: comparison between Japanese and Hungarian. No To Shinkei 1997;49:633–637.

Hyoid Bone Compression–Induced Repetitive Occlusion and Recanalization of the Internal Carotid Artery in a Patient With Ipsilateral Brain and Retinal Ischemia

A 61-YEAR-OLD MAN presented with aphasia and right hemiparesis. Severe stenosis of the left internal carotid artery (ICA) was found 2 years previously when he presented with left retinal arterial branch occlusion. Brain magnetic resonance angiography, carotid ultrasonography (US), and cerebral angiography confirmed that the stenosis had progressed to asymptomatic occlusion 1 year before admission (**Figure 1**A). Brain computed tomography revealed an ischemic lesion in the left basal ganglia (**Figure 2**A). However, the left ICA images were confusing; brain magnetic resonance angiography on day 7 indicated left ICA recanalization, whereas carotid US immediately after magnetic resonance angiography showed ICA occlusion with an intraluminal thrombuslike entity (Figure 2B). Cerebral angiography showed recanalization with severe segmental stenosis on day 13 (Figure 1B); the occlusion revealed by magnetic resonance angiography on day 18 was recanalized according to carotid US 1 hour later. Carotid US on day 20 initially detected left ICA flow in the supine position that gradually diminished with an intraluminal thrombuslike entity appearing over a period of 20 minutes. Flow was suddenly visualized again after the patient sat up (video; http://www.archneurol.com). The left greater horn of the hyoid bone seemed to compress the narrowest segment of the ICA from behind (video), confirmed by helical computed tomography (Figure 1C). Because secondary atherosclerosis at the site of compression, suspected before surgery, was not observed, the operative procedure was changed from carotid endarterectomy to adhesiotomy from the circumferential tissues and patch formation of the left ICA. The hyoid bone removal was given up because of the technical difficulty. A pathological examination of the arterial wall tissue showed only fibrotic change. The left ICA remained patent after surgery. Antiplatelet therapy, started before surgery, was continued. The patient recovered without sequelae and was discharged on day 41.

Video available online at www.archneurol.com

COMMENT

This is the first article describing frequent occlusion and recanalization of a nonatherothrombotic ICA caused by the hyoid bone, confirmed by neuroimaging. To our knowledge, 2 articles[1,2] have described stroke and/or transient ischemic attack in the presence of ICA compression by the hyoid bone, but neither identified a direct relationship between the ICA compression and ischemia. Carotid US and helical computed tomography were useful for diagnosis in our patient. Hyoid bone compression should be recognized as a rare cause of ICA stenosis.

Mayumi Mori, MD
Haruko Yamamoto, MD, PhD
Masatoshi Koga, MD, PhD
Hideki Okatsu, MD
Yuji Shono, MD
Kazunori Toyoda, MD, PhD
Kenji Fukuda, MD
Koji Iihara, MD, PhD
Naoaki Yamada, MD, PhD
Kazuo Minematsu, MD, PhD

Accepted for Publication: October 5, 2010.
Author Affiliations: Departments of Cerebrovascular Medicine (Drs Mori, Yamamoto, Koga, Okatsu, Shono, Toyoda, and Minematsu), Cerebrovascular Surgery (Drs Fukuda and Iihara), and Radiology and Nuclear Medicine (Dr Yamada), National Cerebral and Cardiovascular Center, Osaka, Japan.
Correspondence: Dr Yamamato, Department of Cerebrovascular Medicine, National Cerebral and Cardiovascular Center, 5-7-1 Fujishirodai, Suita, Osaka 565-8565, Japan (harukoya@hsp.ncvc.go.jp).
Author Contributions: *Study concept and design:* Mori and Yamamoto. *Acquisition of data:* Mori, Koga, Shono, Fukuda, Yamada, and Minematsu. *Analysis and interpretation of data:* Mori, Yamamoto, Okatsu, Toyoda, and Iihara. *Drafting of the manuscript:* Mori, Yamamoto, and Yamada. *Critical revision of the manuscript for important intellectual content:* Yamamoto, Koga, Okatsu, Shono, Toyoda, Fukuda, Iihara, and Minematsu. *Obtained funding:* Minematsu. *Administrative, technical, and material support:* Mori, Yamamoto, Koga, Okatsu, Shono, Toyoda, Fukuda, Iihara, and Yamada. *Study supervision:* Minematsu.
Financial Disclosure: None reported.
Funding/Support: This study was supported by Grants-in-Aid (H21-Junkanki-Ippan-017; Dr Minematsu, Chief Investigator) from the Ministry of Health, Labor and Welfare, Japan.
Online-Only Material: The video is available at http://www.archneurol.com.

REFERENCES

1. Abdelaziz OS, Ogilvy CS, Lev M. Is there a potential role for hyoid bone compression in pathogenesis of carotid artery stenosis? *Surg Neurol.* 1999; 51(6):650-653.
2. Kölbel T, Holst J, Lindh M, Mätzsch T. Carotid artery entrapment by the hyoid bone. *J Vasc Surg.* 2008;48(4):1022-1024.

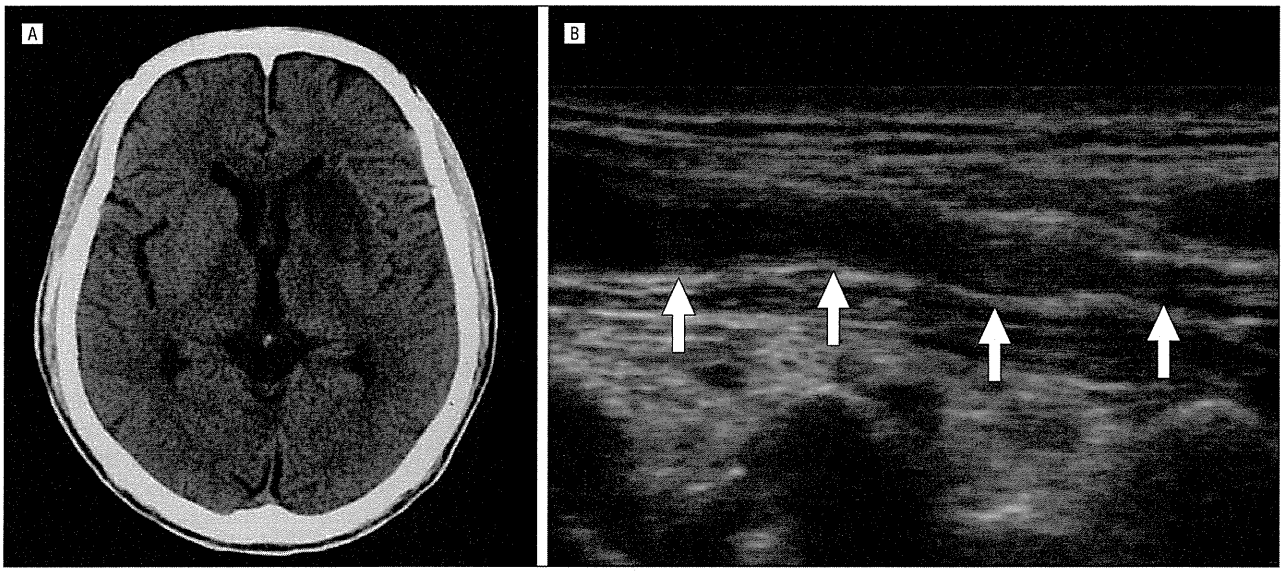

Figure 1. Imaging findings on admission. A, Brain computed tomography shows an ischemic lesion in the left basal ganglia. B, Carotid ultrasound shows a thrombuslike entity in left internal carotid artery.

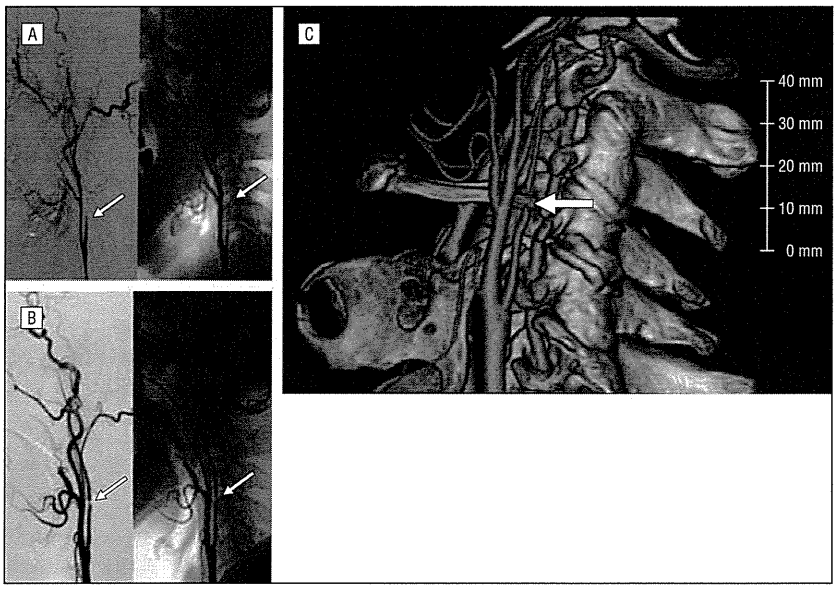

Figure 2. Imaging findings of the left internal carotid artery and hyoid bone. Cerebral angiography showed occlusion of the internal carotid artery 1 year before admission (A), recanalized, with severe segmental stenosis on day 13 (B). C, Helical computed tomography shows the greater horn of hyoid bone compressing the narrowest segment of the left internal carotid artery from behind.

Medical Practice

2011 vol. 28 no. 4

脳卒中診療の新しい展開へのアプローチ
その1
実地医家のための脳卒中診療の新しい展開

脳梗塞急性期治療の新しい展開

古賀政利・峰松一夫

東京 文光堂 本郷

脳卒中診療の新しい展開へのアプローチ
その1
実地医家のための脳卒中診療の新しい展開

脳梗塞急性期治療の新しい展開

古賀政利・峰松一夫*
国立循環器病研究センター脳卒中集中治療科・*同　副院長／こが・まさとし　みねまつ・かずお

はじめに

わが国も本格的な脳卒中急性期治療の時代に突入した．2005年に米国に9年遅れて急性期虚血性脳血管障害の治療薬として承認されたアルテプラーゼ(recombinant tissue-type plasminogen activator, rt-PA)静注療法は，J-MARSなどの患者登録研究によりその安全性と有効性が確認された．この治療法が起爆剤となり，急性期脳卒中への積極的対処の重要性の認識が高まり，一般市民や救急隊を含めた救急医療システムの再構築が進行中である．本稿では，承認から5年経過したrt-PA静注療法の治療成績を概説する．次に，一昨年改訂された脳卒中治療ガイドライン2009における脳梗塞・TIAの急性期治療の主な改訂点や，最近特に注目されているTIA診療の要点を述べる．最後に，注目されている新規治療法を紹介する．

rt-PA静注療法を核とした急性期治療とその成果

1. 国立循環器病研究センターにおける治療成績

当センターでは2010年11月までに，215名にrt-PA静注療法を施行した．2007年12月までの27ヵ月間に当施設に入院しrt-PA静注療法を受けた94例の検討では[1]，同期間に急性期虚血性脳血管障害で入院した948例の約10%，発症3時間以内に入院した333例の28%がこの治療を受けていた．3時間以内に受診した脳梗塞患者の半数以上は，来院時点で軽症であったか，来院後1時間以内に軽症化したため，rt-PA静注療法を行わなかった．発症前にmRS≧2などの16例を除外した78例の解析では，心原性脳塞栓症が51%を占めた．神経学的重症度NIHSSスコアは治療開始前12点(中央値)から24時間後の9点，3週間後3点へと改善した．NIHSSスコアが24時間後に8点以上改善したのは24%で，36時間以内の症候性頭蓋内出血は5%であった．3ヵ月後の完全自立(mRS≦1)は46%で，死亡は2%であった．多変量解析では，3ヵ月後の転帰不良(mRS≧2)の要因は，MRI拡散強調画像上のASPECTSスコアが6点以下，および内頸動脈閉塞であった．当センターの成績は比較的良好であったが，治験への参加などである程度十分な経験を持っていたこと，若手医療者の養成機関としてマンパワーに恵まれ医師も看護師も治療に専念できたこと，心臓内科との連携が良く心不全などの合併症に良く対応できたことなどがその理由と考えられた．

2. SAMURAI rt-PA患者登録研究

厚生労働科学研究費補助金による「わが国における脳卒中再発予防のための急性期内科治療戦略の確立に関する研究」(SAMURAI研究，主任研究者 豊田一則)の一環として，研究班員が所属している脳卒中基幹10施設共同で2005年10月から2008年7月までにrt-PA静注療法を受けた

0910-1551/11/ ¥100/頁 /JCOPY